

Preprint 9, 2014

P.N. Lebedev Physical Institute of the Russian Academy of Sciences

The FAKERAT Software in the International Interferometric Project RADIOASTRON with Very Long Space-Ground Baselines

V.I. Zhuravlev

*Astro Space Center, Lebedev Physical Institute, Russian Academy of Sciences,
Profsoyznaya str. 84/32, Moscow 117997, Russia
zhur@asc.rssi.ru*

March 2014

Abstract

We present the description of the FAKERAT software developed for planning Very Long Baseline Interferometry observations from space (space-VLBI). The results of the planned observations using the FAKERAT package during the first two years after launch of the space radio telescope (SRT) in the space-ground interferometer modes are reported.

1 Introduction

During the first two years the space radio observatory was operated according to the Early Science Program (ESP) of the RadioAstron project [Avdeev et.al. 2012, Kardashev et.al. 2013]. During that stage, the FAKERAT software was tested along with testing the on-board scientific complex. This software may be of interest to potential users who wish to simulate RadioAstron observation, taking into account structural constraints on spacecraft (SC) orientation. Science observations with the RadioAstron SRT are possible only when communication with the ground tracking station¹ for data transfer and frequency synchronization is in operation. These constraints may make it impossible for SRT to observe a given source under certain conditions. As a result of simulating, the information about the possibility of carrying out interferometric sessions for each particular object may be taken. The simulation takes into account the details of the defined scientific task, observation duration, observation date, wavelength range, projection of the interferometer baseline and (u,v)-coverage.

FAKERAT is based on the programs included into "Caltech VLBI Analysis Program" package developed by T.J. Pearson (Caltech) in 1979 in order to support planning and analysis of interferometric observations in experiments with ground baselines. In 1983 D.L. Meier (NASA Jet Propulsion Laboratory (JPL)), added the ability to simulate space VLBI experiments as part of the QUASAT mission development. The software was further developed by D.W. Murphy (JPL) [Murphy 1991, Murphy 2006]. He introduced functional constraints for the space radio telescope VSOP specifically designed for interferometry and added graphical interface. Graphical interface significantly simplified the work related to the experiment planning and analysis of scientific perspectives on interferometric observations. During that stage of software development the FAKESAT package was created. The software was written in FORTRAN and runs on both SUN and HP workstations. It should be relatively easy implemented for UNIX platforms.

In spring of 2011, half a year before RadioAstron launch, we modified FAKESAT taking into account necessary constraints and other peculiarities of the RadioAstron project. Modification included the full replacement of the orbital block. In new orbital block we considered perturbation of orbital elements,

¹In order to transfer data in the interferometric mode during ESP stage, only one highly-informative radio channel (HIRC) of the tracking station prepared in Puschino based on RT-22 radio telescope was used. When this paper was written the second HIRC was prepared on 43 m equatorial radio telescope in NRAO.

introduced new functional constraints specified by orientation SC, the ground tracking and scientific data acquisition station and changed graphical interface to make software more easy to use.

Binary and source code of the modified version known as FAKERAT² is available on the ASC FIAN website³. Installation and usage instructions can be found in RadioAstron User Handbook⁴.

2 Orbital Motion of the Spacecraft

In FAKERAT, the orbital motion of the spacecraft is described by the table of x, y, z coordinate values and components of v_x, v_y, v_z velocity vector in the geocentric coordinate system. Geocentric coordinates and orbital velocities as a function of time are calculated in Keldysh Institute of Applied Mathematics, Russian Academy of Sciences (IAM RAN).

Orbital motion depends on external forces acting on the spacecraft. Not all orbit perturbations including influence of the Sun and Moon are defined a priori with fine precision. The deviation can also arise under the influence of the forces generated by the equipment of SC. For example, it appears due to reactive forces of stabilizing system engines when unloading gyroscopes. Therefore, approximately once every 2-3 months IAM RAN provides new refined tabular values of coordinates and velocities for SC. It is also important to specify orbit after its correction. Fortunately, such manipulations with SC should be done seldom.

In order to get response of an interferometer, it is necessary to know the most precise values of SC coordinates and velocities. It is not an easy task, and, as a rule, orbital calculation for the correlator is limited by the duration of the observations. Positional accuracy of reconstructed orbit for the data processing in the correlator must be no worse than ± 500 m and velocity accuracy no worse than ± 2 cm/c in the three coordinates. More detailed information about orbit reconstruction can be found in [Avdeev et.al. 2012, Kardashev et.al. 2013]. Accuracy requirements for orbital elements in FAKERAT package are by 1.5-2 times less. It allows us to make prediction of the orbit for 5-6 years ahead, which is especially important for planning future observations.

The calculation of the evolution of six orbital elements until the middle of 2019 is shown in Fig. 1. We can see, that due to the impact of the perturbations the length of the major semi-axis changes from 170000 km to 200000 km, eccentricity - from 0.57 to 0.97, and orbit inclination - from $0^\circ.4$ to 84° .

There are several derived parameters: $a(1+e)$ is the orbit apocenter, $a(1-e)$ is the orbit pericenter, and P is the rotation period. The rotation period with known the length of the major semi-axis is given by:

$$P = 2\pi a^{3/2} / \sqrt{\mu} \quad (1)$$

where $\mu = 3.986 \cdot 10^5 \text{ km}^3/\text{c}^2$ is a coefficient equal to the product of the gravitational constant and the Earth mass.

According to the Equation (1) and prediction model of the evolution of orbital elements given in Fig. 1, rotation period will vary from 8.3 to 9.2 days until 2017, and after 2017 its maximum value will increase up to 10.2 days.

The table of coordinate values and components of velocity vector is necessary for FAKERAT to know SC coordinates and velocities at intermediate time points relative to their tabulated values. To obtain such values, we approximate orbit using ellipse with the center of gravity of the Earth at one of its focuses. Here we took into consideration that values of x, y, z, v_x, v_y and v_z at any point of the orbit identically related to the solution of Kepler's equation. Each new line of the table gives new improved orbital approximation. Major semi-axis of an ellipse, eccentricity, ellipse orientation in space, and also SC localization on the orbit were defined by six above-mentioned values. Orbital plane is defined by the orbit inclination and longitude of the ascending node. Pericenter is defined by the angular distance from the ascending node to the orbital pericenter in the direction of SC motion. Timing is defined by moment of passing SC through the pericenter. Angular distance of any point in the orbit is defined relative to the pericenter:

$$u = \omega + \theta$$

where θ is the true anomaly of this arbitrary point. And finally, form and size of the orbit are defined by the major semi-axis and the eccentricity.

²The name of package contains word "FAKE" (from FAKESAT) and also abbreviation of name of RadioAsTron project. Alternatively, it literally means (from English) "fake rat", i.o. an unreal creature object in the Universe to find out the truth.

³<http://www.asc.rssi.ru/radioastron/software/soft.html>

⁴RadioAstron User Handbook, 2012: <http://www.asc.rssi.ru/radioastron/documents/en/rauh.pdf>

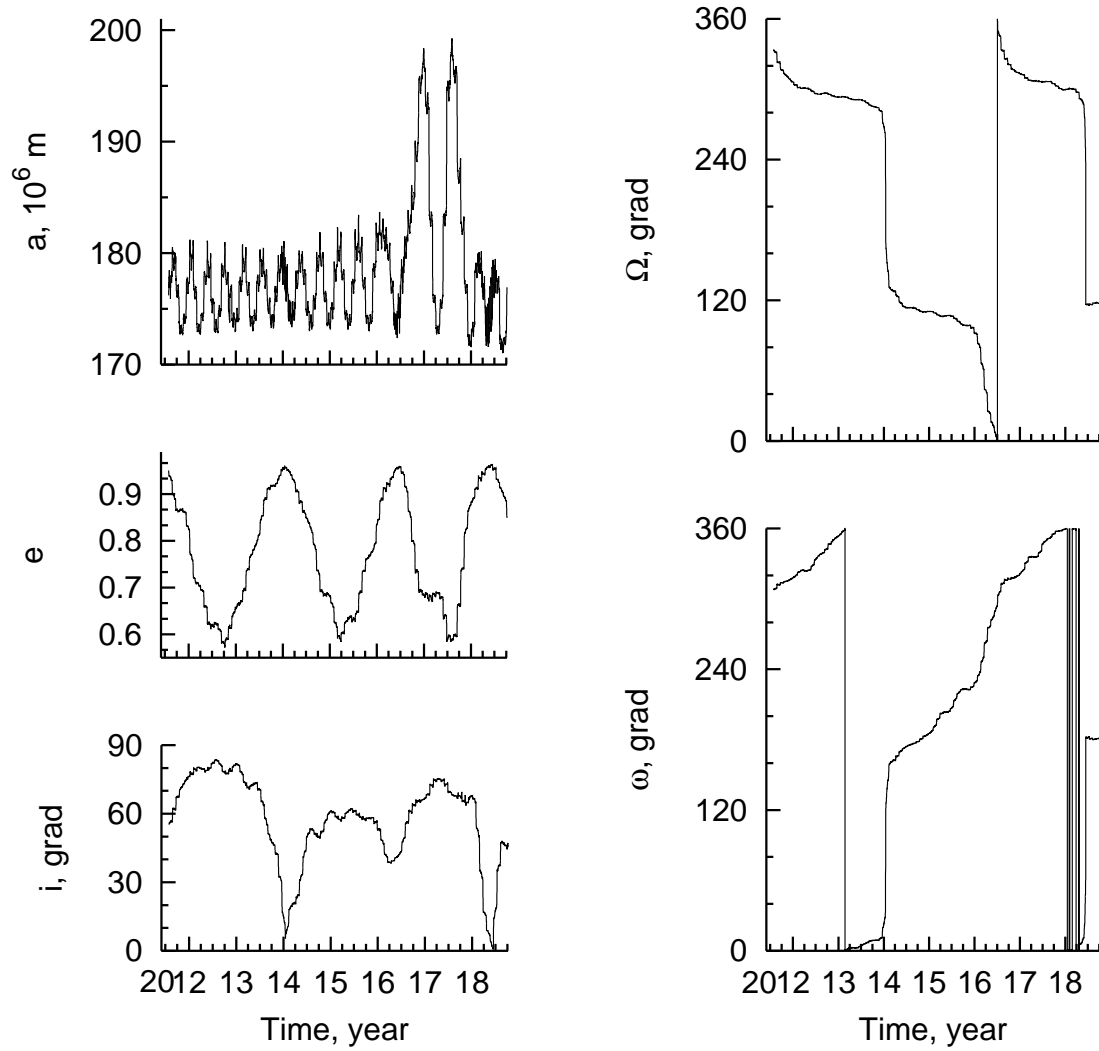
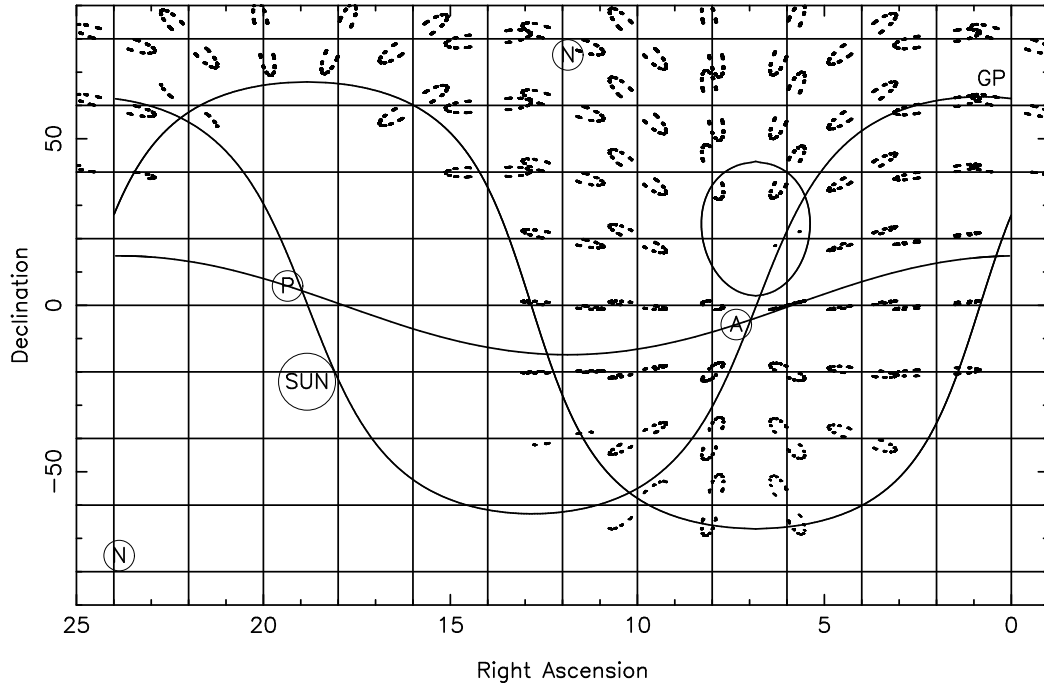


Figure 1: The variations of orbital elements in several years: - semi-major axis (top, left), - eccentricity (left, middle), i - inclination angle (an angle between the orbit plane and the equatorial plane (bottom left), Ω - right ascension of the ascending node (top, right), and ω - angle between the ascending node and the perigee (bottom, right).

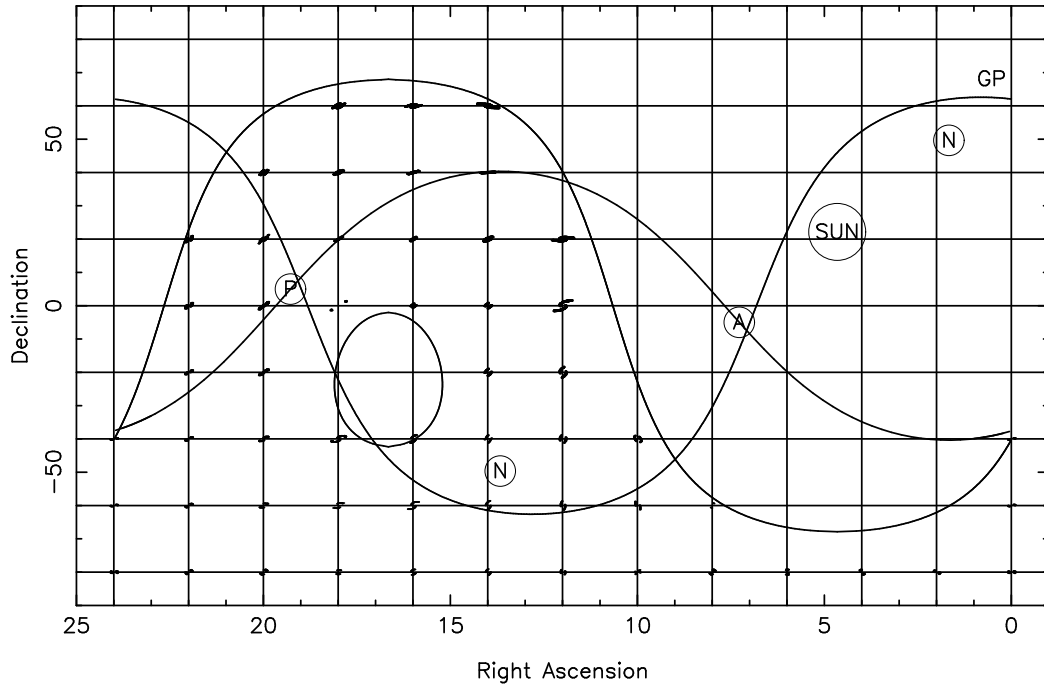
RASTRON;2014;d2 (Jan 2014, 5.000 GHz)
 RASTRON ARECIBO VLA-1 GBT JODRELL EVAPTORI PARKES KALAYZIN USUDA NOTO SHANGHAI BADARY HARDB



Spacecraft Orbital Elements at 0 hr UT on Start Date: (a e i Ω ω M)						
RASTRON	178252129.5	0.956	14.845	267.880	23.135	0.443
defaults file: def-all-c-2014-d2-rastron.2						

24-Apr-2013 16:46

RASTRON;2014;d153 (Jun 2014, 5.000 GHz)
 RASTRON ARECIBO VLA-1 GBT JODRELL EVAPTORI PARKES KALAYZIN USUDA NOTO SHANGHAI BADARY HARDB



Spacecraft Orbital Elements at 0 hr UT on Start Date: (a e i Ω ω M)						
RASTRON	180114417.6	0.873	40.359	115.015	172.298	238.928
defaults file: def-all-c-2014-d153-rastron						

24-Apr-2013 16:52

Figure 2: An example of the all-sky (u,v)-plots at the moment favorable for observation when the Sun is in the lower part of the celestial sphere (top) and at the moment when the Sun is in the upper part of the celestial sphere (bottom).

Filling (u,v)-coverage is mostly defined by the values of the orbital elements. High-elliptical orbit was chosen in order to get ultra-high angular resolution of the objects. The decrease in the degree of filling (u,v)-coverage was supposed to be compensated by orbital evolution under the influence of perturbation from Sun and Moon. It is worthwhile to say that maximum angular resolution is achieved in the direction of normal line towards the orbit plane (see Fig. 2). Coordinates of normal lines for the northern and southern celestial hemisphere are defined by the following expressions: $(\Omega-90^\circ, 90^\circ-i)$ and $(\Omega+90^\circ, i-90^\circ)$ respectively. Sources in the areas close to the normal line towards the plane in the southern celestial hemisphere are rarely observed due to the functional constraints.

In Fig. 2 normal lines towards the plane are marked as \textcircled{N} . In observations of radio sources in the areas close to the normal line, (u,v)-tracks have elliptical structure. This structure contains big gaps. Due to orbit evolution the same sources may be located at one epoch close to the normal, and at other epoch close to the orbit plane. As a result gaps in (u,v)-tracks can be reduced. This reduction takes place due to the simultaneous degradation of angular resolution of the source. In extreme case, when the source is in the orbital plane, i.e. if the distance from the source to the normal line is 90° , (u,v)-tracks have linear structure. A more detailed description of Fig. 2 will be given below.

3 Spacecraft Constraints

There are a number of constraints for SC which make technically impossible to provide observations. Those constraints are given below.

3.1 Thermal Constraints

Observations are not permitted:

- if the angle between SRT electric axis (X) and direction towards SUN center is less than 90° ;
- if the angle between SRT electric axis and direction towards SUN center is more than 165° ;
- if the distance from Earth center to SC is less than 20000 km and a radio source is located at the angular distance less than 30° from the center of Earth's disk.

3.2 Constraints Connected with the Solar Battery Panel

The angle between the normal to the solar panels plane and the direction to the Sun must not exceed 10° . Solar panels can be rotated around the rotation Y-axis only.

3.3 Constraints Connected with the Earth and the Moon.

Observations are not permitted:

- if the distance from the radio source to the nearest edge of the Earth is less than 5° ;
- if the distance from the radio source to the center of the Moon's disk is less than 5° .

3.4 Constraints Connected with Star Sensors

On-board control system includes three star sensors (AX1, AX2 and AX3). In normal mode, only two of them are required. The optical axes of two star sensors (AX1) and (AX2) are placed in the semi-plane turned around the axis parallel to the rotation axis of the solar battery panel (Y) at 15° from the semi-plane YOZ in the direction -X axis, and angle between the AX1 and the -OY axes is 45° and the same angle exist between the AX2 and the +OY axes. The axis of the third star sensor (AX3) is located in the semi-plane XOZ with an inclination from the -X axis by 30° in the direction of the -Z axis.

The defined above coordinate system is right-handed and orthogonal.

According to the measurements made by the Lavochkin Scientific and Production Association (SPA) in July 2012, the star sensors coordinates in the SRT system have next directional cosines:

AX1:	-0.86640913	-0.00055799	-0.499933447
AX2:	-0.18425467	-0.70842875	-0.68130677
AX3:	-0.18282000	0.70791153	-0.68223024

The angle between the axes of each of the two working star sensors and an interfering celestial body should exceed: for Sun - 40° (from the Sun center); for Moon - 30° (from the Moon center); for Earth - 30° (from the nearest edge of Earth).

3.5 Constraints Connected with High-Gain Communication Antenna (HGCA) "Board-Earth"

HGCA provides communication with the ground tracking station (GTS) in order to transfer scientific and service information, and also enables frequency synchronization. Radio source can be observed only in case if such connection exists. Initial angular position GTS relative to the STR coordinate system is defined by the directional cosines:

X axis	-0.95585102	-0.00818895	0.29373758
Y axis	-0.00960202	0.99994823	-0.00336890
Z axis	-0.29369479	-0.00604064	-0.95588015

3.5.1 Algorithm for Calculating HGCA Drive Guidance Angles

When calculating ψ and ϑ angles, anyone should take into account δ_1 and δ_2 angles of the actual electric axis of HGCA. Where δ_1 – angular deviation of HGCA electric axis from the plane XOY and δ_2 – angular deviation of HGCA electric axis onto the plane XOY from "OX" axis. Positive direction of δ_1 is towards "-OZ" axis and positive direction of δ_2 is towards "OY". When drive angles (ψ and ϑ) are equal to zero $\delta_1=14^\circ.67$ and $\delta_2=0^\circ$.

Let us assume that r is a unit radius-vector of GTS point in the on-board coordinate system. Then the following algorithm is implemented:

$$\psi = \text{atan2}\left(\frac{-r_z}{\sqrt{1-r_y^2}}, \frac{r_x}{\sqrt{1-r_y^2}}\right) - \arcsin\left(\frac{\sin \delta_1}{\sqrt{1-r_y^2}}\right)$$

$$\vartheta = \arcsin\left(\frac{r_y}{\cos \delta_1}\right) - \delta_2$$

and condition according to which ψ and ϑ angles belong to the operating range is checked:

$$-75^\circ \leq \psi \leq 90^\circ; 90^\circ \leq \vartheta \leq 90^\circ.$$

The right-handed coordinate system is accepted for positive direction of HGCA drive rotation.

3.6 Constraints Connected with the Ground Tracking and Scientific Data Acquisition Station

Scientific and service information in the project RadioAstron is received by means of 22 meter ground radio telescope of the Puschino Radio Astronomical Observatory (PRAO). The radio telescope should ensure that SRT tracking is performed during the communication session. As it was mentioned above, now it is possible to use the ground tracking station Green Bank with the 43-m radio telescope.

Permitted range of GTS rotation angles in Puschino was specified during ESP: azimuth A - from 6° to 354° and height h - from 10° to 84°.

Permitted range of 43 m radio telescope limited azimuth angles from 82°.5 to 277°.5 and the height must be greater than 11°.

4 Season Variations of Available Sky Area

Fig. 3 shows twelve areas for observations on the celestial sphere in increments of one month. In order to receive this image, we scanned the celestial sphere with a step in right ascension 30 minute and declination – 4°. The possibility of making observations using RadioAstron spacecraft and co-observing ground radio telescopes (Table 1) for each node was checked. Necessary integration time was at least one hour.

We note that area accessible for observation decreases when Sun moves from the southern to the northern hemisphere. This is primarily due to the functional constraints, providing normal thermal conditions, and the possibility of HGCA pointing to the ground tracking antenna.

As it is shown in this figure, some sources can be observed only at the specific time of year and repeated observations are possible again in a year. According to FAKERAT, the northern sources can be observed within 3-4 months/year, and southern - only within 2 months/year or less.

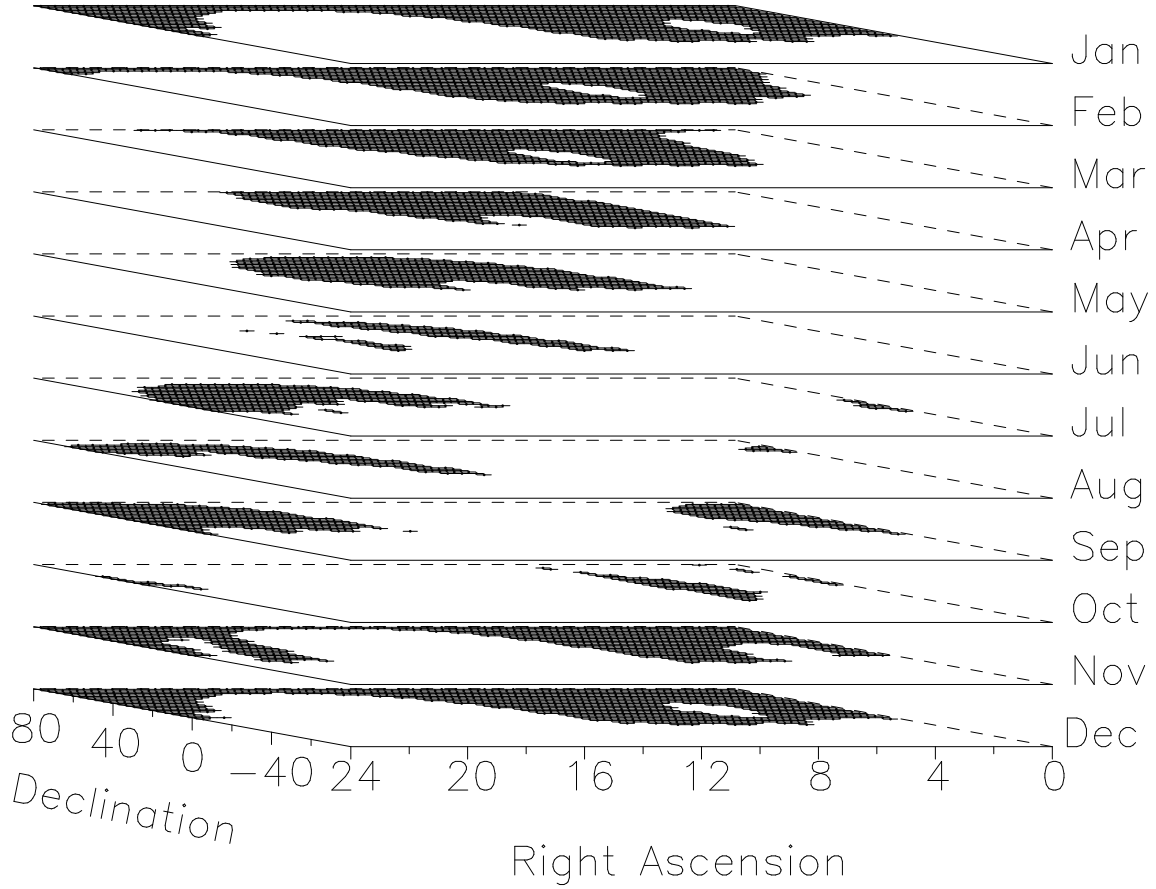


Figure 3: Areas available for observation (dark regions) located according to the months within 2014.

5 Strategy of Using FAKERAT Package

At the present time FAKERAT with graphical interface is working on Linux workstations. To start FAKERAT it is necessary to run Shell script which set environment variables required for running libraries of PGPLOT graphical package. An X Window dialog box will appear for the user to run FAKERAT software. All entered parameters by means of the graphical interface are saved and transferred to the other programs, the copy of which is stored in **menu_defaults.1** file. After starting FAKERAT a user has a number of possibilities for simulate VLBI ground-space observations. First two years of working with FAKERAT showed that the most popular options are follows: (u,v)-coverage as a function of right ascension and declination the whole celestial sphere for a given epoch (**all-sky uvplot**), time evolution of (u,v)-coverage for a given source, at equally intervals time (**time-uvplot**), image of (u,v)-coverage for given source (**uvplot**), and test constrains on date planning observations (**constraints**).

Below is list of main actions that should be performed before modeling VLBI observation:

- connect orbit to the FAKERAT package (i.e. in **orbit** directory of the FAKERAT package should be given a symbolic link **ra_orbit** to the chosen orbit;
- choose a tracking station for data transfer (**tracking station**: PUSCHINO OR GBANK-5);
- set the observation date (**obs-year**, **obs-month** and **obs-day**);
- set the start time of observations (**star hh:mm:ss**);
- set the end time of observations (**stop hh:mm:ss**);
- set the receiver's frequency (**observing band**);
- set the integration time (**τ (s)**);
- specify radio source (**source**);
- set the right ascension (**RA hh:mm:ss.ss**) and declination (**Dec dd:mm:ss.ss**), and

Table 1: List of Ground Radio Telescopes and VLBI Networks participating in space observations.

GRTs/Networks	Diam. (m)	SEFD				Time (%)
		P	L	C	K	
EVN ^a :						
Arecibo (Ar)	305	12	3	5		11
Effelsberg (Eb/Ef)	100	600	19	20	90	51
Hartebeesthoek (Hh)	26		450	795	3000	6
Jodrell Bank (Jb-1)	76	132	65	80		6
Jodrell Bank (Jb-2)	25		320	320	910	2
Medicina (Mc)	32		700	170	700	31
Metsaehovi (Mh)	14				2608	3
Nanshan (Urumqi, Ur)	25		300	250	850	5
Noto (Nt)	32	980	784	260	800	29
Onsala (On-85)	25		320	600		5
Sheshan (Shanghai, Sh)	25		670	720	1700	4
Torun (Tr)	32		300	220	500	21
Westerbork (Wb)	14x25	150	40	60		26
Yebes (Ys)	40			160	200	50
Badary (Bd)	32		330	200	710	20
Svetloe (Sv)	32		360	250	710	27
Zelenchuck (Zc)	32		300	400	710	26
Robledo (Ro70, DSS63)	70		35		83	17
LBA ^b :						
Narrabri, ATCA (At)	1x22		340	350	530	5
Ceduna (Cd)	30				2500	2
Hobart (Ho)	26		420		1800	5
Mopra (Mp)	22		340	350	900	2
Parkes (Pa)	64		42	110	810	2
Tidbinbilla (Ti, DSS43)	70		23		60	< 1
VLBA ^c :						
VLBA_SC, VLBA_FD, VLBA_PT, VLBA_OV	25	2227	303	210	502	< 1
ASKAP (As)	1x12		?			3
GBT ^d (Gb)	100	11	9	10	27	22
PT-70 (Ev)	70		19	19	110	47
Usuda (Us)	64		69	69	?	4
VLA27 ^e (Y)	1x25		420	310	560	< 1
Warkworth (Ww)	12		?			3
Ooty	530mx30m	?				< 1
KRT RadioAstron	10	19000	3400	10500	30000	100

^ahttp://www.evlbi.org/user_guide/EVNstatus.txt

^bhttp://www.atnf.csiro.au/vlbi/documentation/vlbi_antennas

^c<http://science.nrao.edu/facilities/vlba/docs/manuals/oss2013b>

^d<http://science.nrao.edu/facilities/gbt/proposing/GBTpg.pdf>

^e<http://science.nrao.edu/facilities/vla/docs/manuals/oss2013a/performance/sensitivity>

- choose ground radio telescopes (**telescopes**).

Before starting the work, a user should set the time period when the observation is possible to perform. This task may be done using two options: **all-sky uvplot** and **time-uvplot**. In case if observation is impossible, user can find out the reasons using **constraints** option. Typical (u,v)-coverage of grid points for the all celestial sphere when the Sun is in the northern part and in the southern part of celestial sphere are presented be displayed in Fig. 2. In this examples -band (see below), and GTS in Puschino were used. The list of the ground telescopes is given in the upper part of the each figure. In the figure, you can see the areas of the celestial sphere that are not possible to observe due constraints. The projections of the Galaxy plane (GP) and the SC orbital plane onto the celestial sphere are given. Apocenter and

pericenter of the SC orbit are marked as \textcircled{A} and \textcircled{P} respectively.

Once again, from a comparison of these two figures one can see that, when the Sun is in the northern part of celestial sphere, there are significant constraints connected with both the Sun and on the capability to point HGCA to GTS.

The ground radio telescopes involved into space-VLBI experiments during ESP stage are shown in Table 1. Sensitivity of two radio telescopes in interferometric mode can be estimated as follows:

$$\sigma_{i,j} = 1/\psi \sqrt{SEFD_i SEFD_j / 2B\tau}$$

where ψ is an efficiency factor with respect to the unquantized case, τ is integration time in sec., B is the receiver bandwidth in Hz, $SEFD_{i,j}$ is the system equivalent flux densities for i and j of the radio telescope in Jy, respectively. For combination of levels with one-bit (space radio telescope) and two-bit (ground radio telescope) clipped signals $\xi = 0.67$, and for two two-bit clipped signals (two ground radio telescopes) $\xi = 0.881$. We assumed that signal is registered at the Nyquist frequency. $SEFD$ values are given in Table 1.

6 Frequency Specification of On-board System of Receivers

Receiver complex of SC includes on-board system of four receivers that enables to obtain a signal at four wavelengths. Each receiver (except C-band) has two independent channels with left (LCP) and right (RCP) circular polarization signals. In C frequency ranges can be worked only with one polarization. RadioAstron IF-to-Video converter (Formatter) produces two 16 MHz bands (USB and LSB) in frequency ranges L, C, and K. In P-band, receiver contains the signal only for upper sub-band.

Each frequency channel can receive a signal at one of the two bands, apart from each other at 8 MHz:

- P band, with central frequencies 308 MHz or 316 MHz and 16 MHz bandwidth;
- L-band with central frequencies 1660 MHz or 1668 MHz and 60 MHz bandwidth;
- C-band with central frequencies 4828 MHz or 4836 MHz and 110 MHz bandwidth and
- K-band with central frequencies 22228 MHz or 22236 MHz with eight sub-bands for multifrequency synthesis, with four sub-bands for observations of narrow spectral lines and 150 MHz bandwidth.

Central frequencies of eight sub-bands in K-band for multifrequency synthesis apart from each other at 960 MHz: $F_{-4} = 18388$ MHz or 18396 MHz, $F_{-3} = 19348$ MHz or 19356 MHz, $F_{-2} = 20308$ MHz or 20316 MHz, $F_{-1} = 21268$ MHz or 21276 MHz, $F_0 = 22228$ MHz or 22236 MHz, $F_1 = 23188$ MHz or 23196 MHz, $F_2 = 24148$ MHz or 24156 MHz and $F_3 = 25108$ MHz or 25116 MHz.

Central frequencies of four sub-bands in K-band for spectral observations apart from each other at 32 MHz: $F_0 = 22228$ MHz or 22236 MHz, $F_{0-1} = 22196$ MHz or 22204 MHz, $F_{0-2} = 22164$ MHz or 22172 MHz and $F_{0-3} = 22132$ MHz or 22140 MHz. More information about the work of on-board scientific complex a user can find in work [Kardashev et.al. 2013].

The FAKERAT package provides the ability to calculate of (u,v)-coverage for frequency syntheses in K-band using 8 sub-bands from 1.19 to 1.63 cm. Fig. 6f-6k of the work [Kardashev et.al. 2013] show examples of the corresponding evolution of K-band (u,v)-coverage for two edge sub-bands for 2013, 2014 and 2015, for the radio galaxy M87 and Cen A involving SRT and eight ground radio telescopes (Green Bank, Goldstone, Effelsberg, Jodrell Bank, Evpatoria, Parkes, Tidbinbilla, and Robledo). Significant ellipticity observed in the (u,v)-coverage can be reduced in the future using orbit correction.

7 Conclusion

About 600 interferometric sessions of RadioAstron project at all four operational wavelengths were planned and successfully observed by the end of June 2013. All planning was done using FAKERAT package, including the first test observations of the Moon. When Moon observation was planned, some SC functional constraints in the FAKERAT package have been violated. Total time of the scientific observations during this period was more than 712 hours.

Acknowledgments. The RadioAstron project is led by the Astro Space Center of the Lebedev Physical Institute of the Russian Academy of Sciences and the Lavochkin Scientific and Production Association under a contract with the Russian Federal Space Agency, in collaboration with partner organizations in Russia and other countries. The author would like to thank Russian and foreign colleagues participating in FAKERAT package development: A.V. Alakoz, M.V. Popov and V.A. Soglasnov for online testing package, K.V. Sokolovsky for testing package in automatic mode without using graphical interface, Yu.Yu. Kovalev for developing network version of the package, E.B. Kravchenko and J.M. Anderson (Max Planck Institute for Radio Astronomy, German) for the revision of the archive of the ground radio telescopes, P.A. Voytsik and C.R. Gwinn (University of California Santa Barbara, USA) for conversion of the package into 64-bit version and distribution of that version among IBM PC and Apple users, V.G. Promyslov for accommodation of FAKESAT at PC-platform, V.E. Yakimov for placing the package on ASC FIAN website, and T.S. Fetisova for scientific editing of the paper. In particular, the author would like to thank D.W. Murphy (JPL) for its participation in RadioAstron project. Due to that participation effective software for planning observations in the space-VLBI international interferometric experiment was developed within the shortest possible time.

References

- [Avdeev et.al. 2012] Avdeev V.Yu. et al., 2012, Vestn. FGUP NPO im. S.A.Lavochkina, 4
- [Kardashev et.al. 2013] Kardashev N.S. et al. ARep, 2013, 57, 153
- [Murphy 1991] D.W. Murphy, Simulations of space VLBI, Radio interferometry: Theory, techniques, and applications; Proceedings of the 131st IAU Colloquium, ASP Conference Series (ASP: San Francisco), 1991, vol. 19, p. 107
- [Murphy 2006] Murphy D.W., VSOP-2 Mission Simulations Using the JPL-developed Fakesat Software, 36th COSPAR Scientific Assembly. Held 16-23 July in Beijing, China, 2006, P.2496